Mesenchymal stem cells cultivated on scaffolds formed by 3D printed PCL matrices, coated with PLGA electrospun nanofibers for use in tissue engineering

Mesenchymal stem cells cultivated on scaffolds formed by 3D printed PCL matrices, coated with PLGA electrospun nanofibers for use in tissue engineering

Natasha Maurmann[1,2], Daniela P. Pereira[1], Daniela Burguez[1], Frederico D. A. de S. Pereira[3], Paulo Inforçatti Neto[3], Rodrigo A. Rezende[3], Douglas Gamba[4], Jorge V. L. da Silva[3], and Patricia Pranke[1,2,5]

[1] Hematology and Stem Cell Laboratory, Faculty of Pharmacy, Universidade Federal do Rio Grande do Sul (UFRGS), Porto Alegre, Brazil.

[2] Post-graduation program in Phisiology, UFRGS, Porto Alegre, Brazil.

[3] Division of 3D Technologies – Centre for Information Technology Renato Archer, Campinas, Brazil.

[4] Institute of Chemistry, UFRGS, Porto Alegre, Brazil.

[5] Instituto de Pesquisa com Células-tronco, Porto Alegre, Brazil.

Abstract

Materials, such as biopolymers, can be applied to produce scaffolds as mechanical support for cell growth in regenerative medicine. Two examples are polycaprolactone (PCL) and poly (lactic-*co*-glycolic acid) (PLGA), both used in this study to evaluate the behaviour of umbilical cord-derived mesenchymal stem cells (UCMSC). The scaffolds were produced by the 3D printing technique using PCL as a polymer covered with PLGA fibers obtained by electrospinning. The cells were seeded in three concentrations: 8.5 x 10^3; 25.5 x 10^3 and 51.0 x 10^3 on the two surfaces of the scaffolds. With scanning electron microscopy (SEM), it was observed that the electrospun fibers were integrated into the 3D printed matrices. Confocal laser scanning microscopy and SEM confirmed the presence of attached cells and the lactate dehydrogenase release test showed the scaffolds were not cytotoxic. The cells were able to differentiate into osteogenic and chondrogenic lineages on the scaffolds. Mechanical test showed that the cells seeded on the 3D printed PCL matrices coated with PLGA electrospun nanofibers (3D+ES+SC) did not show significant difference in tensile modulus than the pure

PCL matrix (3D) or PCL matrices coated with PLGA electrospun nanofibers (3D+ES). The combination of the two polymers facilitated the production of a support with greater mechanical stability due to the presence of the 3D printed PCL matrices fabricated by melted filaments and greater cell adhesion due to the PLGA fibers. The scaffolds are suitable for use in cell therapy and also for tissue regeneration purposes.

1. Introduction

Tissue engineering (TE) has attracted considerable attention in recent years as a promising area of medicine for reconstructing and replacing damaged organs and tissue. Regenerative medicine combines the principles of engineering and biology for the development of biomaterials, using scaffolds and cells for tissue regeneration (Langer and Vacanti 1993; Chan and Leong 2008).

Ideally, scaffolds used in TE have several requirements that characterize a successful approach, including particular biological, mechanical, physical and chemical ones (Dhandayuthapani *et al* 2011). These are:

(a) biocompatibility, supporting cell growth and maintenance, with a negligible immune reaction (Dhandayuthapani *et al* 2011; Hussein *et al* 2016; Rana *et al* 2015; O'Brien 2011; Teo *et al* 2006; Skardal and Atala 2015);

(b) provision of appropriate structural support, shape and mechanical stability for the cells, including stiffness and swelling consistent with the anatomical site into which they are to be implanted and with sufficient strength to allow surgical handling during implantation (Chan and Leong 2008; Dhandayuthapani *et al* 2011; O'Brien 2011; Teo *et al* 2006; Hollister 2005; Giannitelli *et al* 2015);

(c) architecture with interconnected pore structure and porosity to ensure cellular adhesion, penetration, engraftment and migration, adequate diffusion of nutrients to cells, gas exchange (i.e., O_2 and CO_2), metabolic waste removal, and signal transduction because the microenvironment can create additional sites for cell anchorage and may provide distinct biochemical cues to guide cell behavior (Dhandayuthapani *et al* 2011; Rana *et al* 2015; O'Brien 2011; Hollister 2005; Giannitelli *et al* 2015);

(d) surface properties, e.g., ability to conduct signals, surface energy, chemistry, charge, surface area and suitable surface finishing;

(e) biodegradability, with a degradation rate in synchrony with defect healing rate (Dhandayuthapani *et al* 2011; Rana *et al* 2015; O'Brien 2011; Minuth *et al* 2005);

(f) sterilization facility because scaffolds are implanted into medical devices and as such are required to meet stringent sterility regulations to ensure patient safety (Baume *et al* 2016);

(g) in addition to physical and spatial cues, the scaffold itself can be the carrier of signaling biomolecules, thus emphasizing the need for scaffold-based tissue engineering (Rana *et al* 2015).

The requirements to be taken into account when leading with a scaffold can be seen in figure 1.

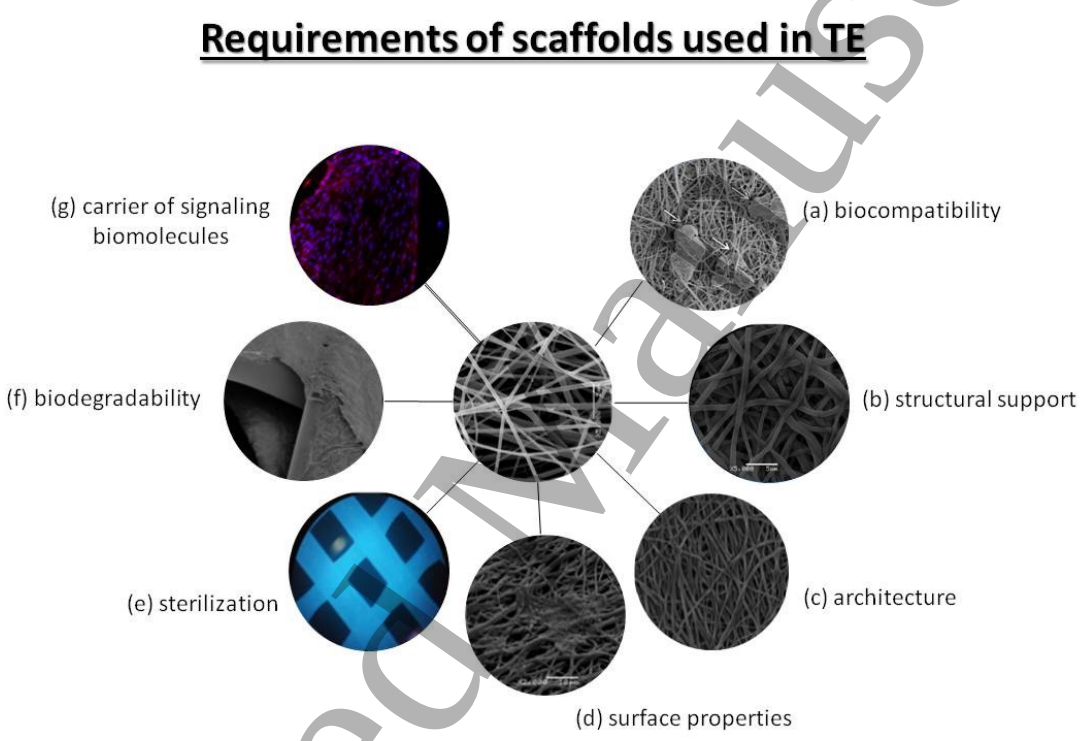

Figure 1. Some requirements of a scaffold used in TE: (a) biocompatibility, (b) structural support, (c) architecture, (d) surface properties, (e) sterilization, (f) biodegradability and (g) carrier of signaling biomolecules.

Modern technologies exist which may be used to produce scaffolds based on biomaterials processed by additive manufacturing (AM). There is a wide range of areas where AM is applied and medicine (health) is one of the fastest growing areas. Furthermore, there is substantial research focused on obtaining future autologous implantable tissue and organs through 3D printing (Skardal and Atala 2015).

The consolidated technique called electrospinning facilitates the manufacturing of nanostructured fibers with dimensions similar to components in the extracellular matrix, mimicking its fibrillar structure and providing essential cues for cellular organization, survival and function (Dhandayuthapani *et al* 2011). A typical electrospinning set up is shown in figure 2a. Electrospinning and additive manufacturing are technologies that converge toward the same goal and can complement each other. They are independently applied sciences for manufacturing scaffolds for a variety of tissue engineering applications (Dalton *et al* 2013).

Many types of biomaterials can be used to produce scaffolds for tissue engineering (Dhandayuthapani *et al* 2011; Teo *et al* 2006; Ulery *et al* 2011). Aliphatic polyesters, such as polycaprolactone (PCL) and poly(lactide-*co*-glycolide) (PLGA), have excellent tissue compatibility and degradability, which are critical aspects for their successful use in the human body. Moreover, these polymers have been approved by the United States Food and Drug Administration (FDA) and European Medicine Agency (EMA) for biomedical applications (Ulery *et al* 2011).

Mesenchymal stem or stromal cells (MSC) serve as a fundamental part of tissue engineering. These cells areoften used in combination with biomaterials with the aim of repairing or reconstructing tissue and organs (Langer and Vacanti 1993). MSC are multipotent cells found in a variety of human tissue and organs (Ullah *et al* 2015; Kang *et al* 2012). They contribute to the regeneration of many types of tissue and organs, such as bone, cartilage, muscle**,** ligament, tendon, adipose tissue, stroma and fibrous tissue (Kang *et al* 2012). Besides their aptitude for tissue replacement via multipotent differentiation, MSC have been recognized for their therapeutic immunomodulatory and anti-inflammatory effects and also for the secretion of molecules or bioactive factors that instigate or assist in tissue repair (Lavoie and Rosu-Myles 2013; Paul and Anisimovc 2013). Among the non-invasive sources to obtain MSC, human umbilical cord is an interesting source as the umbilical cord is normally discarded after birth. Favorable characteristics of human umbilical cord mesenchymal stem cells (UCMSC) include good differentiation and proliferation capabilities (Baksh *et al* 2007; Kern *et al* 2006).

The present study has investigated the interaction between biomaterials and MSC. The scaffolds were produced through 3D printing to manufacture 3D PCL matrices with suitable mechanical properties covered by electrospun PLGA to improve cell attachment (figure 2).

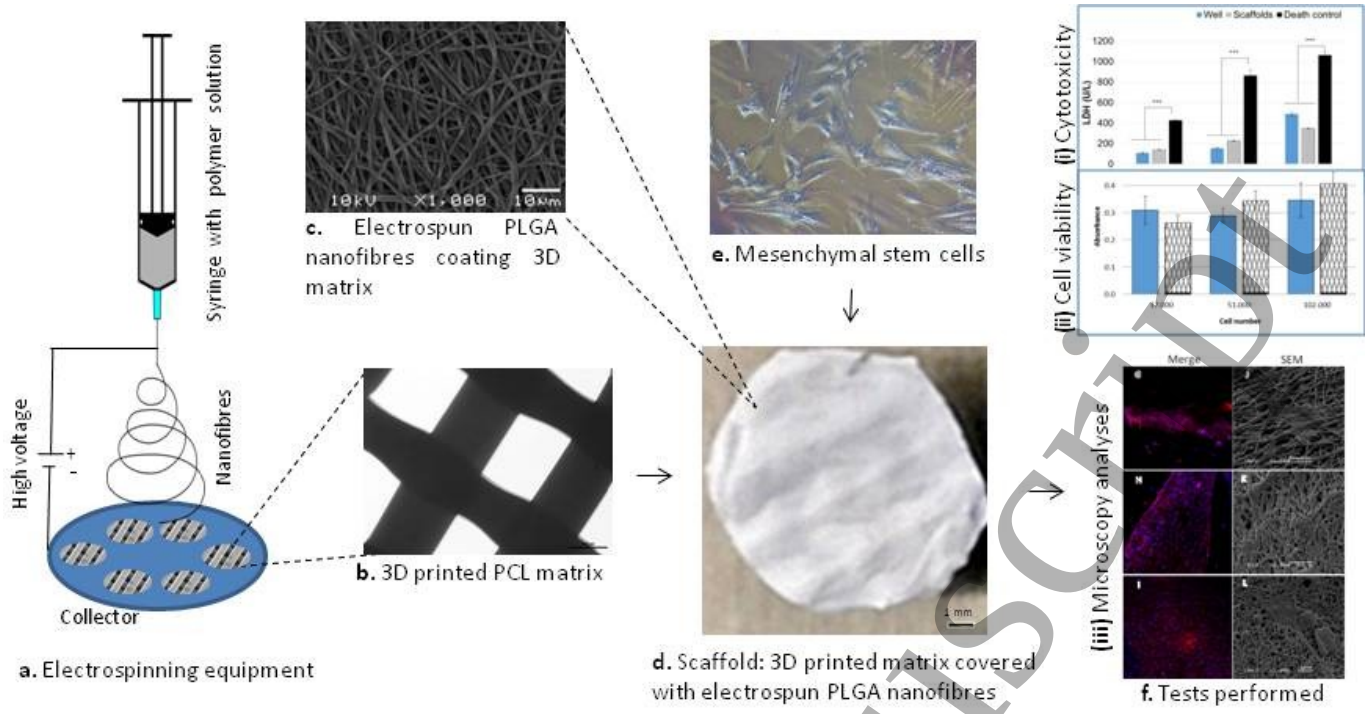

Figure 2. Summary of the experiments. Panel (a) shows a schematic diagram of the electrospinning setup used in this study. (b) Printed PCL matrix. (c) Electrospun PLGA nanofibers coating 3D matrix. (d) Scaffolds composed of PCL 3D printed matrix covered with electrospun PLGA nanofibers. (e) Mesenchymal stem cells from umbilical cord seeded on the scaffolds. (f) Summary of the tests performed with MSC seeded at 17 x 10^3, 51 x 10^3 and 102 x 10^3: (i) cytotoxicity assessed by measuring the culture supernatant using enzyme lactate dehydrogenase (LDH) delivery assay; (ii) cell viability determined using MTT assay and (iii) confocal laser scanning microscopy of merge staining with DAPI (blue nuclei) and phalloidin (red cytoskeleton) images (left) and scanning electron microscopy of the cells and the PLGA fibers (right).

2. Materials and methods

2.1. Materials

The products used were heat-inactivated Fetal Bovine Serum (FBS) (Cultilab, Campinas/SP), collagenase type I and penicillin/streptomycin (Gibco), LDH Liquiform Ref.: 86-1/100 (Labtest Diagnóstica SA), OCT compound (Sakura). The surface markers used were: CD14, CD29, CD34, CD45, CD90, CD105 and HLA-DR (Becton Dickinson, San Diego, CA) and growth factor Rh-TGF-β-1 (Peprotech). The polymers used were poly(DL-lactide-co-glycolide) 75/25 (PLGA) (PURAC) and polycaprolactone (PCL) (Solvay Capa 6505). The following products were purchased from Sigma-Aldrich: Dulbecco's Modified Eagle's Medium (DMEM/HEPES) – low glucose, amphotericin B, 3-(4,5-dimethylthiazol-2-yl)-2,5-diphenyltetrasolium bromide (MTT), trypsin-EDTA solution 10x, dimethyl sulphoxide (DMSO), dexamethasone, L-ascorbic acid 2-phosphate sesquimagnesium salt hydrate (ASAP), ITS Liquid Media Supplement (100x), alcian blue 8GX, insulin from bovine pancreas, indomethacin minimum, rosiglitazone, oil red O, β-glycerophosphate disodium salt hydrate, alizarin red S and Triton X-100. TRIizol® Reagent and Power SYBR® Green qPCR Master Mix kit were purchased from Life Technologies and M-MLV Reverse Transcriptase kit, actin, osteocalcin and osteopontin were purchased from Invitrogen.

2.2. Hybrid fabrication: 3D Printing plus electrospinning

The poly(lactic-*co*-glycolic acid) (PLGA) fibers were deposited by an electrospinning apparatus onto printed PCL matrices to improve the biofouling of the MSC on the scaffolds.

2.2.1. 3D Printed PCL matrices

The PCL matrices (porous woodpile-like structures, figure 2b) were fabricated by the 3D printing process with the 3D printer, Fab@CTI (figure 3a), which consisted of the extrusion of fused filaments (Lixandrão *et al* 2009). The most common hydroplastic forming technique is extrusion, in which a stiff plastic ceramic mass is forced through a die orifice,

having the desired cross-sectional geometry. A forming technique is applied whereby a material is forced by compression through a die orifice. The extrusion process is the molding of a viscous thermoplastic under pressure through an open-ended die. A mechanical screw or auger propels the pelletized material through a chamber, which is then compacted, melted, and formed into a continuous charge of viscous fluid. The technique is especially adapted for producing continuous lengths, having constant cross-sectional geometries—for example, rods, tubes, hose channels, sheets, and filaments (Callister 2007). Scaffolds can also be fabricated in the same way.

The scaffolds were printed with 2 layers, each of 0.4 mm, and cut in circular forms with diameters of approximately 6 mm. The PCL printed matrices were produced with a 1 mm air gap, which refers to the space found between the raster lines. The Fab@CTI was built and adapted at the Center for Information Technology Renato Archer (CTI) with the purpose of collaborating in research initiatives in the bioengineering and biomaterials fields through partnerships with many research institutions. Fab@CTI can use materials under different conditions, such as filament, powder and fluid state.

The printer head (figure 3b) used in this work has the potential of being adapted to different filament diameters and different melting temperatures (room temperature to 400°C) (Inforçatti Neto *et al* 2011).

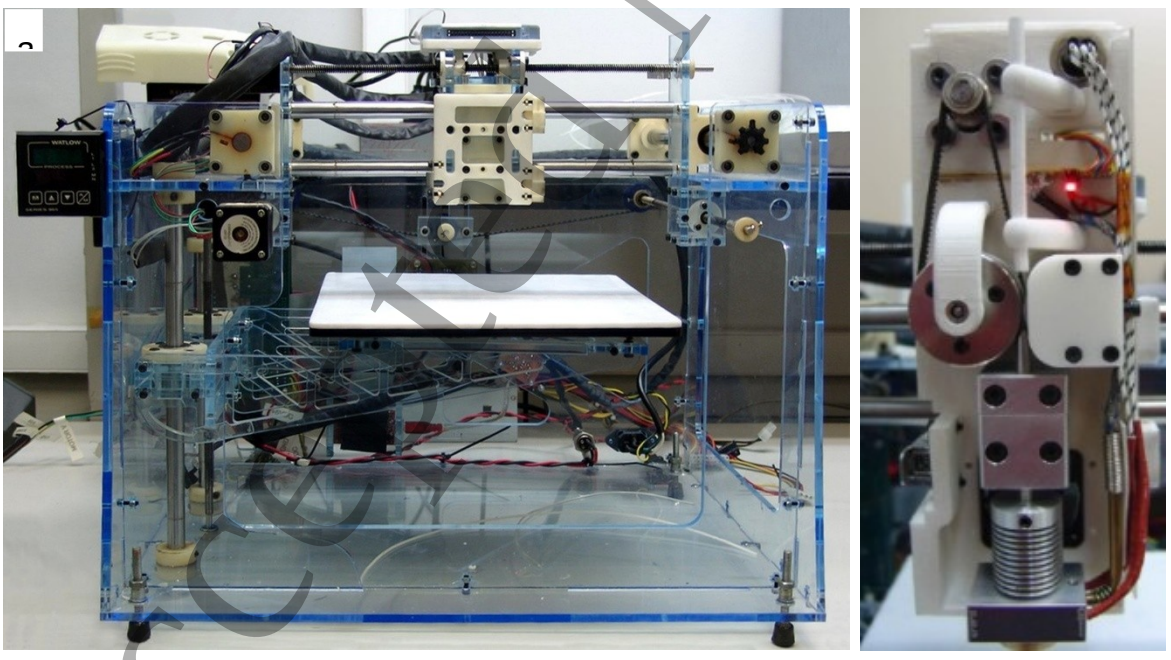

Figure 3. Fab@CTI (a) and the printer head developed at CTI Renato Archer for extruding thermoplastics polymeric filaments (b).

2.2.2. Electrospun PLGA coating

PLGA was used for electrospinning, as previously described (Acasigua *et al* 2014). 12% PLGA (75/25) was dissolved in 1,1,1,3,3,3-hexafluoro-2-propanol. The polymer solutions were placed between electrodes connected to a high voltage. The voltages applied for the nanofiber production were 11 kV and 1 kV, corresponding to the positive and negative electrodes, respectively. The polymer solution was electrospun with a syringe equipped with a 21G x1" steel needle (0.8 x 25 mm), at 15 cm distance from the stationary collector plate with a flow rate of 0.019 mL/min (Acasigua *et al* 2014). Random fibers were electrospun on a collector containing PCL with 6 mm diameter on both sides of the 3D matrices (figure 2a). 0.45 mL of the PLGA polymer solution was used on each side of the 3D matrices, forming the 3D+ES scaffolds (figure 2d). Subsequently, the 3D+ES scaffolds were placed under ultraviolet light for 1.5 hours in a vertical laminar flow hood (45 minutes for each side) for sterilization and then placed in 96 well culture plates.

2.3. Umbilical cord mesenchymal stem cells (UCMSC) isolated from humans

2.3.1. Cell isolation

The samples of the umbilical cord were obtained in partnership with the *Hospital Moinhos de Vento de Porto Alegre*, Brazil. This work was approved by the Research Ethics Committees of the Pharmacy School/*Universidade Federal do Rio Grande do Sul* (protocol number 27315) and by the Brazil Platform Committee for Ethics and Research, called *Plataforma Brasil*. This program is under the auspice of the Ministry of Health for the registration of studies involving humans, based on the opinion of the Certificate of Presentation for Ethical Consideration (CAAE- *Certificado de Apresentação para Apreciação Ética*) under number 36211214.3.0000.5347. Participants were informed regarding the objectives and procedures of the study and signed a consent form.

The umbilical cord was harvested after birth. Immediately after collection, the umbilical cord was immersed in MSC culture medium, consisting of DMEM/Hepes, pH 7.4 supplemented with 10% FBS, 100 U/mL penicillin, 100 µg/mL streptomycin and 0.25

µg/mL amphotericin. The umbilical cord was cut in a laminar flow, washed with phosphate buffered saline (PBS) and Wharton's jelly from the umbilical cord was digested in a 0.1% solution of collagenase type I. The cells were seeded into a culture bottle (T75 cm^2). The medium was replaced after 24 hours in order to isolate adherent cells and, thereafter, it was refreshed once every 3 days to allow further growth. The cells were maintained at 37°C in a humidified atmosphere containing 5% CO_2. After reaching confluence, the cells were detached with trypsin–EDTA 0.05% solution and re-seeded at a density of 5,000 cells/cm^2 until they reached the 6^{th} passage for characterization and use in the experiments described below.

2.3.2. Cell characterization

The UCMSC were characterized by flow cytometry and by the ability to differentiate into osteoblasts, chondrocytes and adipocytes *in vitro* (Acasigua *et al* 2014; Andrade *et al* 2016).

2.3.2.1. Immunophenotypic profile by flow cytometry

The immunophenotypic profile of the MSC was performed after cell dissociation with Trypsin/EDTA and posterior incubation with specific monoclonal antibodies. The cells were counted, re-suspended in PBS buffer at 10^6 cells/mL and incubated with the human antibodies. The positive markers were CD29, CD90 and CD105 and the negative markers were CD14, CD34, CD45 and HLA-DR. The antibodies were conjugated with fluorescein isothiocyanate (FITC), phycoerythrin (PE) or allophycocyanin (APC). After 30 minutes incubation in the dark, the cells were washed with PBS to remove unbound antibody excess. Appropriate isotype controls were used and exclusion of dead cells was performed by incubation with 7-aminoactinomycin D (7AAD). The analyses were performed by flow cytometer FACSAria III (Becton Dickinson) and analyzed by FACSDiva software, version 6.0 (Acasigua *et al* 2014, Andrade *et al* 2016).

2.3.2.2. Cell differentiation *in vitro*

The cell cultures were evaluated for their capacity to differentiate into osteoblasts, chondrocytes and adipocytes through induction medium until acquiring morphological

change for about one month, as detailed below. The cells were fixed with 4% paraformaldehyde. The photomicrographs were captured by an optical microscope, as previously described (Acasigua *et al* 2014, Andrade *et al* 2016).

2.3.2.2.1. Adipogenic differentiation

The cells were cultivated in MSC culture medium supplemented with dexamethasone (1 µM), insulin (10 µg/ml), indomethacin (50 µM), rosiglitazone (1 µM) and IBMX (0.5 mM). The deposits of lipid droplets were observed after oil red O staining.

2.3.2.2.2. Chondrogenic differentiation

For chondrogenic differentiation, the cells were cultivated in differentiation medium for about 30 days. The inducing medium consisted of MSC culture medium supplemented with 10 ng/mL TGF-β 1, 0.1 µM dexamethasone, 50 nM solution of ascorbic acid 2-phosphate (ASAP) and 1x of ITS 100x. The chondrogenesis was made apparent by alcian blue staining.

2.3.2.2.3. Osteogenic differentiation

The cells were cultivated for 3-4 weeks in a supplemented MSC culture medium containing dexamethasone (0.1 µM), ascorbic acid 2-phosphate (5 µM) and β-glycerophosphate (15 mM). The deposition of the mineralized matrix was observed by alizarin red S staining.

2.3.2.2.4. Control

The cells were cultivated in MSC culture medium in the same plates for the same time as the cells treated with a differentiation induction medium. After change in the cell morphology in the differentiation cultures, the MSC (control) were fixed and stained with each of the three different dyes at the end of each differentiation, as described above.

2.3.3. Cell cultivation in the scaffolds

The UCMSC were seeded in three concentrations: 8.5 x 10^3; 25.5 x 10^3 and 51.0 x 10^3 on one of the surfaces of the 3D+ES scaffolds. The 96-well culture plates without scaffolds were used as control. After 48 hours, the scaffolds were turned over and the same number of cells was seeded on the other surface of the scaffolds, totaling 1.7 x 10^4, 5.1 x 10^4 and 10.2 x 10^4 UCMSC seeded for the treatment in scaffolds and in the controls wells. After a further 48 hours, the tests were considered completed.

2.4. Cytotoxicity assay

Cytotoxicity was assessed by measuring the culture supernatant using enzyme lactate dehydrogenase (LDH) delivery assay. It is an intracellular enzyme and its increased presence in the extracellular environment is indicative of problems in the cytoplasmic membrane integrity and, consequently, provoking cell damage. The higher the concentration of this enzyme, the higher the cell death. The test (Labtest kit) was performed 48 h after the second seeding. As negative control, cells cultivated directly on the wells were used and as positive control, cells cultivated directly on the wells treated with Triton X-100 (Sigma-Aldrich), 1% (v/v) for 20 minutes. Triton X-100 causes cell death, permitting maximal LDH release. Measurement was performed with the equipment 560 Labmax (Labtest Diagnóstica SA) (Andrade *et al* 2016). Data is means ± SEM for three experiments (n = 12 for treatment).

2.5. Cell viability (MTT assay)

Cell viability was determined using the colorimetric MTT assay. Two days after the second seeding, the cells were incubated with 0.25 µg/mL MTT; four hours later, the supernatant was carefully removed and DMSO (200 µL) was added per well to dissolve the crystals formed. Absorbance was measured at 570 nm and 630 nm in the apparatus SpectraMax® 250 (Molecular Device, Sunnyvale, CA, USA), with the results being calculated by the absorbance label subtraction (570 nm-630 nm) (Andrade *et al* 2016). Data is means ± SEM for four experiments (n = 14 for treatment).

2.6. Image analysis

2.6.1. Optical microscopy

Both cell differentiation and the PCL matrices were analyzed by the images obtained in a Nikon microscope (Nikon Ti Eclipse microscope). The matrix diameter was determined using the ImageJ program (National Institutes of Health).

2.6.2. Scanning electron microscopy

The scaffold morphology and the PLGA fiber diameter, together with the cell presence were observed by scanning electron microscope Zeiss Evo 50 (Carl-Zeiss, Oberkochen, Germany). Fiber diameter was determined using the ImageJ programme. The scaffolds were washed in phosphate buffer (pH 7.4), fixed in 3% glutaraldehyde buffer for 30 minutes, rinsed in buffer PBS and dehydrated in an ethanol series. Dried samples were metalized with a thin layer of platinum and were placed on stabs using adhesive carbon discs. The images were obtained using accelerating voltage of 10 kV with a magnification range of 1,000-20,000x (Zanatta *et al* 2012).

2.6.3. Confocal laser scanning microscopy

The presence of cells was analyzed by confocal laser scanning microscopy. The samples were washed in phosphate buffer (pH 7.4), fixed in 4% paraphormaldehyde buffer for 20 minutes and rinsed in buffer PBS. The stem cells were permeabilized with Triton X and the actin of the cytoplasms were stained red using 50 µg/mL rhodamine conjugated phalloidin (40 minutes). They were washed with PBS and the cell nuclei were blue stained with 0.5 µg/mL of 4,6-diamidino-2-phenilindole, DAPI (1 minute). Photographs were obtained by confocal-laser scanning fluorescence microscope with an objective of EC Plan-Neofluar 10x/0.30 M27 (Zeiss Model LSM 700) (Zanatta *et al* 2012).

The quantitative analyses of results were made by normalization: the cells attached on the scaffolds and stained with DAPI were counted (cell attachment number) and then normalized in relation to the seeded cell number (cell attachment number/seeded cell number). Three images were used for each cell concentration.

2.6.4. Cell differentiation on the scaffolds

Capacity of osteogenic and chondrogenic differentiation of stem cells was performed on the 3D+ES scaffolds (3D printed PCL matrices coated with PLGA electrospun nanofibers). The UCMSC (51.0 x 10^3) were seeded on one of the surfaces of the scaffolds (3D+ES).

After the differentiation period on the scaffolds (about 2 weeks), the osteogenic differentiation of cells was analyzed by the following methodologies: PCR, alkaline phosphatase activity assay and histology.

Total RNA from the constructs (3D+ES+UCMSC) was extracted using the TRIizol® Reagent method, in accordance with the manufacturer's directions. After 10 days each constructs was washed with PBS, vortexed in 2mL TRIzol® for 5 minutes and stored at -80°C until further use. Proteins were removed with 0.4 mL chloroform extraction, and the RNA pellets were washed once with isopropyl alcohol and once with 75% ethanol. The total number of RNA pellets were reconstituted in diethyl pyrocarbonate-treated water (DEPC). The concentration and purity of the RNA was measured using a NanoDrop (ND-2000) Spectrophotometer. cDNA was synthesized using a moloney murine leukemia virus reverse transcriptase enzyme M-MLV Reverse Transcriptase kit. The single-strand cDNA synthesis occurred by incubating the complete reaction mixture for 5 min at 65°C, followed by ice and 50 min at 37°C and terminated by an incubation at 70°C for 15 min. PCR reactions were prepared using Power SYBR® Green qPCR Master Mix kit. Each 20 µL sample was composed of 10 µL of qPCRSupermix, 1 µL of albumin, 0.5 µM of each primer (Table 1) and 1 µL of cDNA, diluted in DEPC water. PCR cycle conditions were as follows: 95°C for 2 minutes followed by 44 cycles at 95°C for 15sec (denaturation), 30sec of annealing (temperature dependent on the gene, table 1) and 72°C for 30sec (extension) were carried out in an Applied Biosystems® Thermo Cycler. PCR-amplified fragments were resolved by 1.5% agarose/ethidium bromide gel electrophoresis.

Table 1. PCR primers of osteogenic markers.

Gene		Primer sequences (5`–3`)	Tm (°C)
Actin	Sense:	AGCACAGAGCCTCGCCTT	60
	Antisense:	CGGCGATATCATCATCCA	
Osteocalcin	Sense:	GCAGAGTCCAGCAAAGGTGC	61.4
	Antisense:	TCAGCCAACTCGTCAGAGTC	
Osteopontin	Sense:	GCAACCGAAGTTTTCACTCC	58.4
	Antisense:	TGAGGTGATGTCCTCGTCTG	

The scaffolds with differentiated cells were stained for cytoplasmic alkaline phosphatase activity using a commercial alkaline phosphatase live stain detection kit (Life Technologies/ThermoFisher, USA), in accordance with the manufacturer's instructions, and analyzed by fluorescence microscopy.

In the histological analysis of osteogenic differentiation of the cells and the controls of cell-polymer, the constructs were fixed with 4% paraformaldehyde and stained with alizarin red S. The photomicrographs from the whole scaffold with differentiated cells were captured by an optical microscope, as previously described. Cell-polymer constructs were embedded in optimum cutting temperature (OCT) compound and cryosectioned (25 µm thick) in a Slee Cryostat. The photomicrographs were captured by an optical microscope.

The chondrogenic differentiation of cells cultivated on the scaffolds (about 4 weeks) was analyzed by histology after staining with alcian blue, as described above.

2.6.5. Mechanical test

The tensile mechanical properties of the scaffolds were measured using a DMA Q800 (TA Instruments, New Castle, USA). Three different groups were characterized: samples of PCL 3D printed matrix (3D) without nanofibers and cells; 3D scaffolds covered with electrospun PLGA nanofibers (3D+ES) and 3D+ES scaffolds containing stem cells from umbilical cord (3D+ES+SC). The UCMSC were seeded on the surfaces of the 3D+ES scaffolds, equivalent to the highest cell concentration used (corresponding to 51.0 x 10^3/0.32 cm^2). After 48 hours, the scaffolds were turned over and the same number of

cells was seeded on the other surface of the scaffolds. After a further 48 hours, the tests were performed. The analyses of the scaffolds with cells were made immediately after the cultivation time by removing the excess of culture media. The samples were prepared at dimensions of 20 mm x 5 mm x 0.85 mm (l x w x t) and clamped for the tensile mode. The measurements of stress x strain were made at 37°C, with a soak time of 5 minutes and a tensile load of 1 N/min until failure. The Young modulus, tensile at break and elongation at break, were obtained from an average of three measurements of each group using Universal Analysis software (TA Instruments).

2.7. Statistical analysis

The results were expressed as the mean ± standard error of the mean (SEM) and evaluated using one-way ANOVA, followed by Bonferroni's test. Significant differences were established at $p<0.05$. Data analyses were performed with the programme BioEstat 5.0 (Ayres 2007).

3. Results and discussion

3.1. Scaffolds 3D of PCL covered by PLGA electruspun (3D+ES)

Figure 2d shows the macroscopic aspect of the scaffolds produced. It is possible to see the electrospun fibers integrated with the 3D matrices. The aspect of the 3D matrices isshown in figure 4a (optical microscopy). The PCL 3D-printed matrices were constructed with two different layer diameters: at the bottom, the average diameter was 797.5 µm with standard error of 61.0 µm and at the top layer of the matrix it was 581.2 ± 13.9 µm, measured in the centre of the rod. The 3D-printed matrices covered with electrospun PLGA nanofibers can be seen in figure 4b. The SEM of the PLGA nanofibers is shown in figure 4c. It was possible to observe that the fibers were distributed in a random manner over the entire scaffold structure and presented a large number of interconnected pores.

The average diameter of the electrospun PLGA fibers was 109.4 ± 42.7 nm and the histogram in figure 4d illustrates the fiber diameter distribution as a function of frequency (number of fibers that lie in the fiber diameter group). In this study, the produced scaffolds showed a favorable geometry for facilitating their manipulation. Moreover, the

scaffolds exhibited fibers with different nanometric dimensions, interconnected pores and an elevated superficial area.

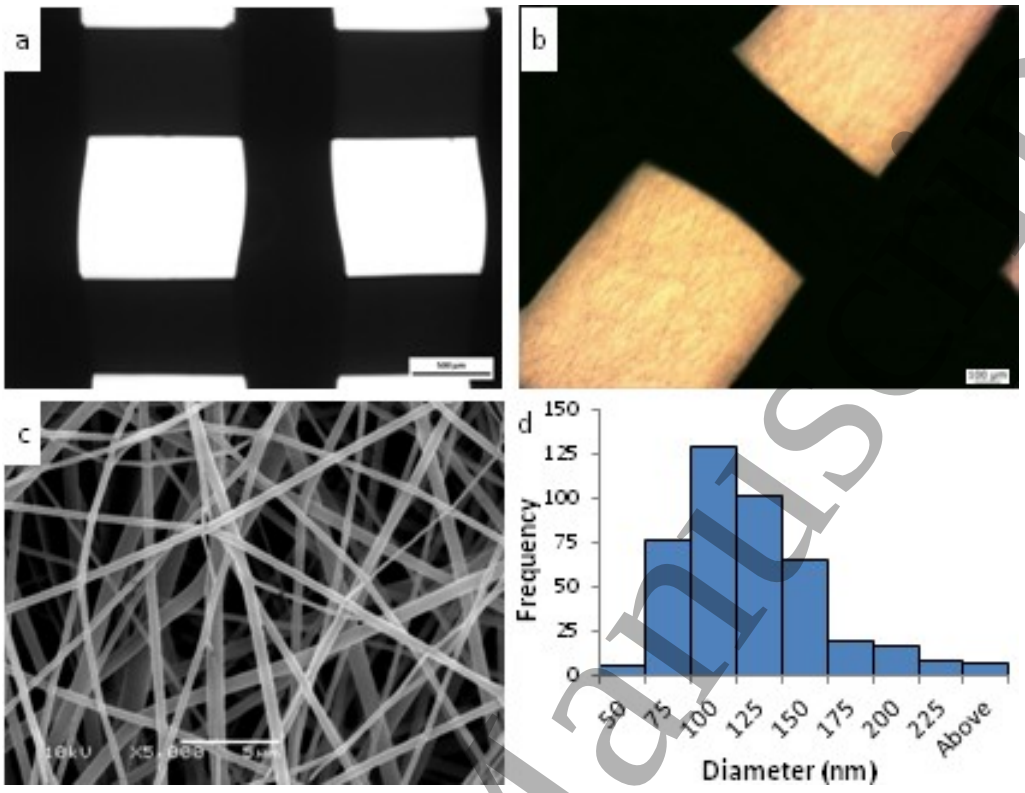

Figure 4. Aspect of (a) PCL 3D-printed matrix by optical microscopy, (b) 3D-printed matrix covered with electrospun nanofibers. (c) PLGA electrospun fibers by SEM and (d) histogram showing PLGA fiber diameter.

The fibers had diameters compatible with the fibers of the natural extracellular matrix (ECM). In the native tissue, the structural ECM proteins range in diameter from 50 to 500 nm (Barnes *et al* 2007). In this work, the diameter of the fibers varied from 34 to 391 nm, with the main concentration of between 75 and 150 nm. Conventional polymer processing techniques have difficulty in producing fibers smaller than 10 μm in diameter, which are several orders of magnitude larger than the native ECM. For this reason, there has been a concerted effort to develop methods for producing nanofibers to more closely simulate the ECM geometry, such as electrospinning (Barnes *et al* 2007). The influence of the ECM on cellular activities occurs via the binding of specific factors to specific ECM molecules and the binding of ECM molecules to cell surface receptors, known as

integrins. The participation of integrin-β1 in MSC adherence on PLGA nanofibers produced by electrospinning has been previously demonstrated (Zanatta *et al* 2012). Integrin-mediated cell adhesion is of substantial importance as it links ECM with cytoskeleton and signal transduction cascade to regulate cell shape, differentiation, adhesion, migration and proliferation in many systems (Schwartz and Assoian 2001).

Moreover, the PLGA electrospun nanofibers produced in previous studies of the group were able to give support to cell differentiation of MSC (Acasigua *et al* 2014, Zanatta *et al* 2012). This behavior is desirable because this system gives enough mechanical support for cellular adherence and spreading, providing adequate material to support differentiation for chondrocyte and ECM production. This system can be used as carrier material in transplantation procedures, allowing MSC to be firmly adhered to the material during the transport to the injured site (Acasigua *et al* 2014).

3.2. Mesenchymal stem cell characterization

The MSC from human umbilical cord were isolated, cultivated and characterized successfully from three different umbilical cords. The cells showed typical MSC morphology, characteristics of plastic adherence, colony forming unit and immunophenotyping showed positivity for the surface markers CD29/PE (figure 5a), CD90/FITC (figure 5b), CD105/APC (figure 5c) (>95%) with low expression for CD14/FITC (figure 5d), CD34/PE (figure 5e), CD45/FITC and HLA-DR/FITC (figure 5f) (<2%).

The cells were able to differentiate into the three analyzed mesodermal cell lineages (osteogenic, adipogenic and chondrogenic). Photomicrographs of a representative sample of the UCMSC from differentiated umbilical cord cultures are shown in figure 5. Adipogenic differentiation was demonstrated by staining with oil red O, without evidence of lipid vacuoles in the control (figure 5h), but showed droplets of fat, highlighted by oil red O (figure 5k). Chondrogenic differentiation was demonstrated by staining with alcian blue, indicated by the blue staining of glycosaminoglycans deposits (figure 5l), but not in the control (figure 5i). Osteogenic differentiation was demonstrated by staining with alizarin red S, indicated by the red staining of the calcium deposits (figure 5m), but without evidence of the calcified matrix stained with alizarin red S in the control (figure 5j).

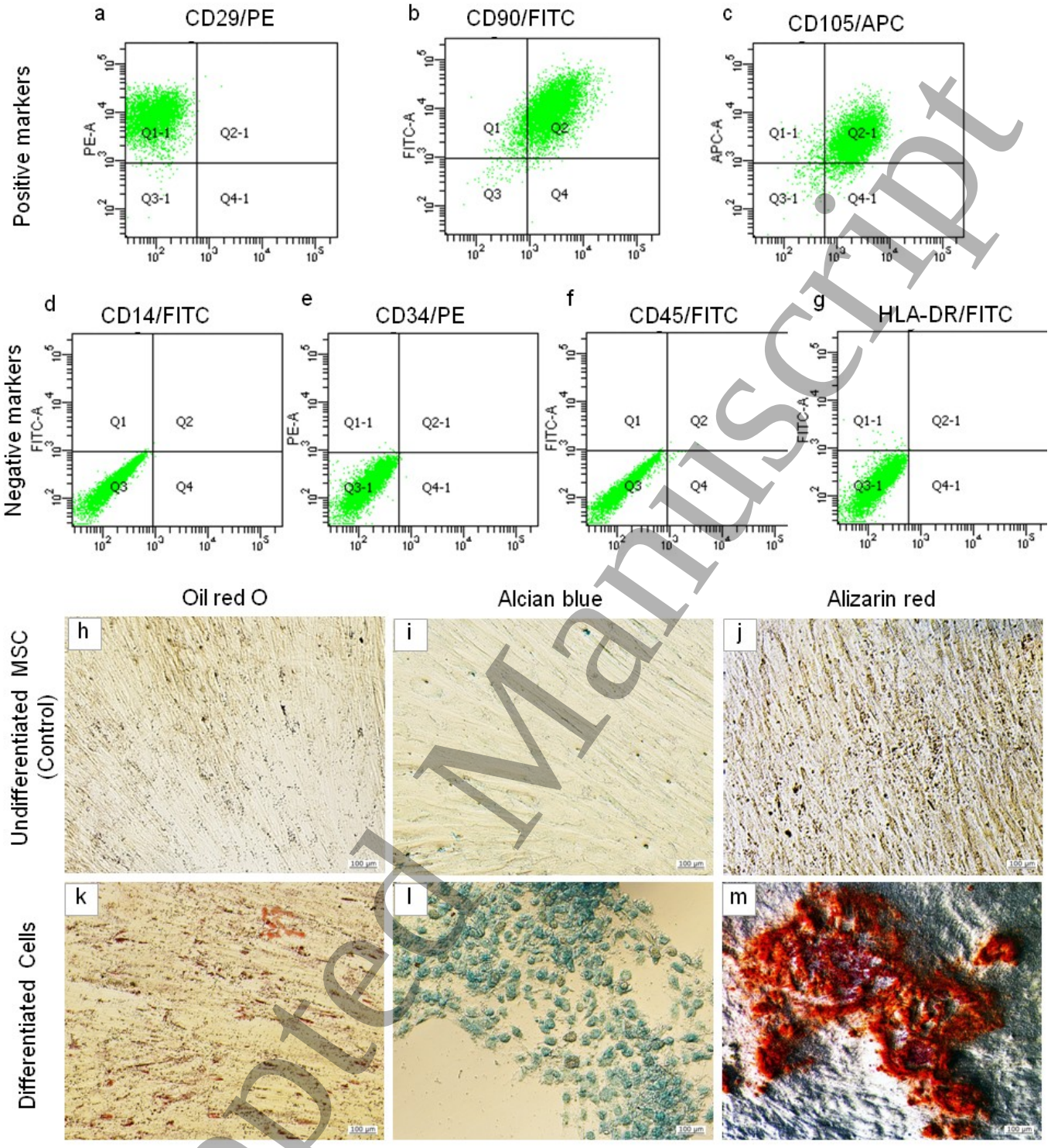

Figure 5. Mesenchymal stem cell characterization. Immunophenotyping showed positivity for the surface markers CD29/PE (a), CD90/FITC (b), CD105/APC (c) (>95%) with low expression for CD14/FITC (d), CD34/PE (e), CD45/FITC and HLA-DR/FITC (g) (<2%). MSC differentiation potential within the three mesodermal lineages. The cells cultivated in MSC medium used as control and stained with oil red O (h), alcian blue (i) and alizarin red S

(j). Differentiation of MSC in the following lineages: (k) adipogenic, (l) chondrogenic and (m) osteogenic, stained with oil red O, alcian blue and alizarin red S, respectively. 100x magnification. Representative photomicrographs from UCMSC of one umbilical cord culture.

In this study, mesenchymal stem cells were characterized following The International Society for Cellular Therapy (ISCT) standard criteria: the cells must be plastic-adherent when maintained in standard culture conditions; MSC must express positivity (≥95%) to CD73 (ecto-5´-nucleotidase), CD90 (Thy1) and CD105 (endoglin), while negatively expressing (≤2%) CD11b or CD14, CD34, CD45 and HLA-DR surface molecules and the MSC must differentiate into osteoblasts, adipocytes and chondroblasts *in vitro* (Dominici *et al* 2006).

Human umbilical cord-derived MSC can be isolated and expanded easily *in vitro* without ethical concerns because the cord is discarded after birth (Cui *et al* 2015, Moretti *et al* 2010). This postnatal organ has been found to be rich in primitive stromal cells, showing typical characteristics of bone-marrow (BM) MSC (BMSC) (Moretti *et al* 2010). Compared to BM, umbilical cord tissue carries a higher frequency of stromal cells with a higher in vitro expansion potential. Therefore, MSC from umbilical cord have attracted interest as a promising candidate for several potential clinical applications due to the immune-privileged and immune-modulatory properties (Moretti *et al* 2010). Thus, MSC from umbilical cord are a powerful cellular alternative for regenerative medicine and tissue engineering applications and open highly interesting perspectives for clinical applications (Moretti *et al* 2010).

3.3. Cytotoxicity assay

The cytotoxicity of the scaffolds of PLGA fiber-coated PCL was evaluated by LDH concentrations measured on the supernatant of the cell culture. The LDH delivery assay showed that the scaffolds were not cytotoxic (figure 6). In the test, with a 17 x 10^3 MSC seeded density, the average

LDH (U/L) released and standard deviation of the control well was 103.1 ± 22.5 and the scaffold was 125.1 ± 36.2. In the death control (Triton) it was 300.2 ± 177.3. At the concentration of 51 x 10^3 cells, the average was 144.6 ± 36.7, 181.2 ± 79.0 and 512.4 ± 369.3, in the control, scaffold and death control groups, respectively. When 102 x 10^3 MSC were seeded in the wells, the average LDH (U/L) released was 327.0 ± 313.7. When seeded on the scaffolds, it was 291.0 ± 168.9 and when seeded in the Triton-treated wells it was 950.9 ± 558.1. No significant statistical difference occurred between the LDH leakage (U/L) in the control (cells cultivated on the plates) and in the 3D+ES scaffolds ($p > 0.05$) with each cell density used. Cells treated with Triton were used as the positive control for cell death and, statistically, they delivered more LDH than the cells cultivated on the plates ($p < 0.05$) and in the scaffolds ($p < 0.05$).

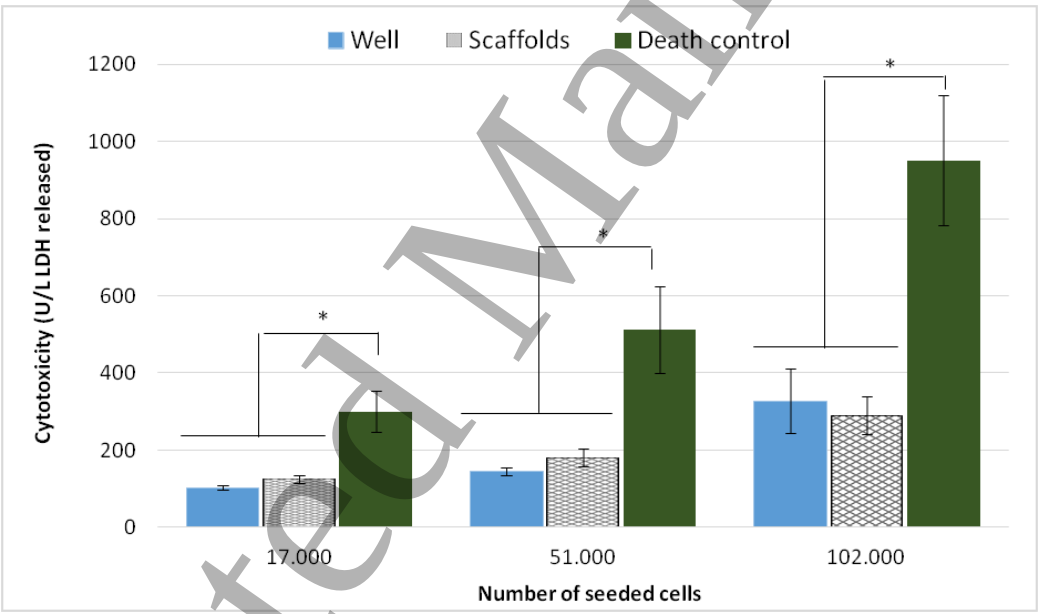

Figure 6. Cytotoxicity of the scaffolds measured by LDH release from the supernatant culture of the UCMSC. The cells were seeded at different densities in the wells (negative control), scaffolds (3D+ES) and the wells treated with Triton (death control). *$p < 0.05$

For clinical success, an ideal scaffold must not release cytotoxic substances but should support growth, adherence and proliferation of the seeded cells (Açil *et al* 2014). In order to evaluate the chemical characteristics of the biomaterials, the cytotoxicity of eluates from the biomaterials was investigated by using the LDH test. The LDH assay is an effective means of measuring the membrane integrity (cytotoxicity) as a function of the amount of leaked LDH, a cytoplasmic enzyme released from injured cells into the medium (Açil *et al* 2014).

The organic chemical solvents used in electrospinning are a source of cytotoxic compounds. For example, most of the polymers used in electrospinning are not soluble in an aqueous media, as, for example, PLGA. Therefore, the use of organic solvents possessing high toxicity is necessary. However, during the electrospinning procedure, the solvent will evaporate as the fluid jet accelerates toward the collector. In this path, if most of the solvent evaporates, individual fibers are formed. If not, the fibers may not be formed at all, or a thin film of polymer solution is deposited on the collector (Ramakrishna *et al* 2005). It was shown that, despite the fact that HFIP residue was present in the PLGA electrospun fibers the amount of retained HFIP was too low to impart any *in vitro* or *in vivo* toxicity (Weldon *et al* 2012). The possible presence of solvent residuals; however, or other interference cannot be excluded and cytotoxicity assay is necessary. The LDH test demonstrated that the tested scaffolds formed by 3D+ES, did not cause an increase of LDH release, which indicates that the scaffolds were not cytotoxic to the MSC.

3.4. Cell viability

MTT is reduced to formazan in viable cells, thus the level of reducing MTT into formazan can reflect the level of cellular metabolism and cell proliferation. After the second seeding, cell viability assay showed that there were no statistically significant differences between the wells and the scaffolds in terms of MSC concentration. In the test with a 17 x 10^3 MSC seeded density, the average absorbance and standard deviation of the control well was 0.31 ± 0.19 and the scaffold was 0.26 ± 0.10. At the

concentration of 51 x 10^3 cells, the absorbance was 0.29 ± 0.10 and 0.35 ± 0.13 in the control and scaffold groups, respectively. When 102 x 10^3 MSC were seeded in the wells (control), the absorbance was 0.35 ± 0.24 and when seeded on the scaffolds, it was 0.41 ± 0.16. It is therefore possible to conclude that the scaffolds behaved similarly to the wells (gold standard).

In high doses of seeded cells (51 x 10^3 and 102 x 10^3 MSC), there was a trend of better viability in the scaffolds. This is possibly due to the approach used in this study to seed cells on both sides of the scaffolds. Thus, the cells on both sides of the scaffolds had more space for growth than in the wells.

Previous studies of the group have demonstrated that MSC from dental pulp of deciduous teeth proliferated in 12% PLGA fibers obtained by electrospinning (Acasigua *et al* 2014). There was an increase in cell viability (by MTT assay) in both groups (PLGA fiber scaffold and plate control) on the 7^{th} day of cultivation when compared to the first day of the experiments. The same occurred on the 14^{th} day when cell viability increased in both groups. However, on the 21^{st} day of cultivation, cell viability decreased in both groups in comparison to the 14^{th} day.

Cell viability remained similar in the test and control groups in the different experiment timeperiods, with no statistical difference between them (Acasigua *et al* 2014). In addition, the study demonstrated that the association of MSC seeded into biodegradable PLGA scaffolds has the ability of promoting bone regeneration in rats, which is a promising alternative for application in regenerative medicine (Acasigua *et al* 2014).

3.5. Interaction of cells with scaffolds

The presence of the cells attached in the scaffolds was confirmed by confocal laser scanning microscopy and scanning electron microscopy. Figure 7 shows the cells with the blue nuclear staining with DAPI on one side of the scaffold with 8.5 x 10^3 (figure 7a), 25.5 x 10^3 (figure 7b) and 51

x 10³ MSC (figure 7c); the red cytoskeletal actin filaments stained with phalloidin, with 8.5 x 10^3 (figure 7d), 25.5 x 10^3 (figure 7E) and 51 x 10³ MSC (figure 7f) and the digital overlay of DAPI and phalloidin, with 8.5 x 10^3 (figure 7G), 25.5 x 10^3 (figure 7h) and 51 x 10³ MSC (figure 7i). The appearance of the cells attached to the PLGA fibers is shown by scanning electron microscopy, with 8.5 x 10^3 (figure 7j), 25.5 x 10^3 (figure 7k) and 51 x 10³ MSC (figure 7l).

Cell attachment on the scaffolds was investigated by staining the cell nucleus using DAPI. The cytoskeletal characteristics were investigated by using phalloidin by fluorescent microscopic and scanning electron microscopy images of the cells on the scaffolds.

The quantitative analyses using normalization of data (number of cells attachment after 4 days they were seeded on the scaffolds in relation to the number of cells seeded at day 0) resulted the rates of 1.78, 1.77 and 1.88 of MSC with 8,500, 25,500 and 51,000 of cells seeded, respectively. The similar ratio in the differents number of cells seeded on the scaffolds (1.78, 1.77 and 1.88) indicates that regardless of the number of cells used to start the experiment (8,500, 25,500 and 51,000), the presented scaffold approach allows for similar cell proliferation. Besides this, the rate greater than 1 suggests a higher cell attachment number in relation to the seeded cell number and indicates cell proliferation on the scaffolds after 4 days in cultivation. This result suggests that the UCMSC can proliferate in the proposed 3D+ES scaffolds used in this work. It was confirmed that the seeding of 51,000 cells resulted in a higher attachment than the 25,500 and 8,500 cells seeded on each side of the scaffold, with similar proliferation rates. Consistent with the cell attachment results by fluorescent microscopic, the SEM on the 51,000 cell seeding manifested the largest number of cells.

In general, the experiments use 2 x 10^4 to 3 x 10^4 plated cells per cm^2 and allow proliferation and performing analyses at different points in the growth curve. This approach has been used in previous experiments of the group in scaffolds with 12% PLGA and MSC with analysis at 7, 14 and

21 days (Acasigua *et al* 2014). In the present study, the lower cell density used (8.5 x 10^3 cells per well in 96 well plates) corresponds to this interval (2.6 x 10^4 cells per cm^2). At this density, it is possible to observe spaces without cells in the scaffolds (figure 7a, d, g). The cells use these spaces to proliferate in experiments of longer duration. The higher density MSC seeded approach in this work was used to reduce the time of the experiment.

After four days of experiments, it can be concluded that the 51,000 seeded cells are suitable for transplant to the scaffold because the cells have a confluent layer on the scaffold (figure 7c, f, i).

A different approach of seeding cells on both sides of the scaffolds was used with the aim of increasing cell density. Thus, it is possible to have stem cells on both sides of the scaffold when transplanting this material to injured tissue, presumably accelerating the regeneration time.

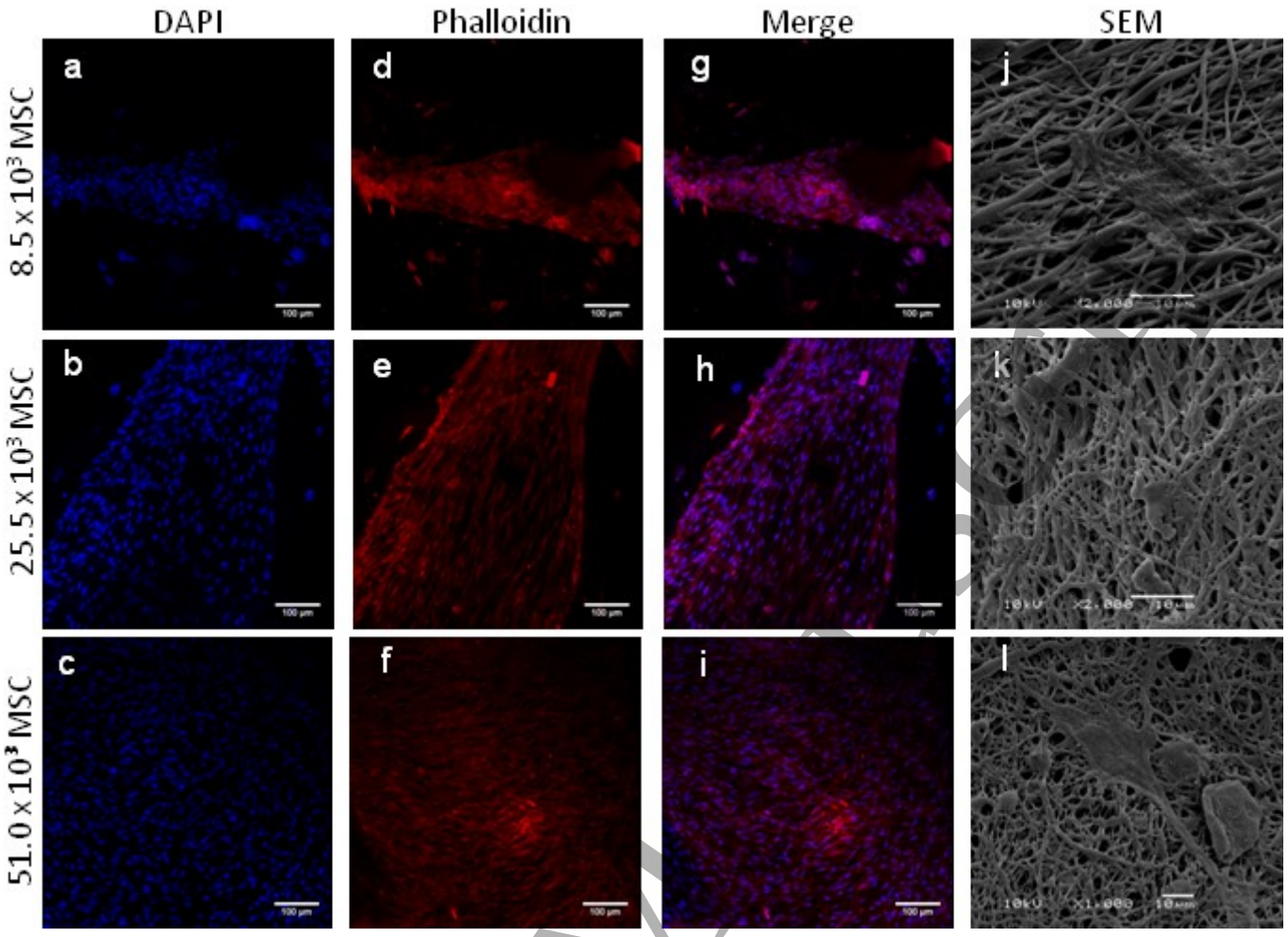

Figure 7. Confocal laser scanning microscopy of MSC seeding density with 8.5 x 10^3, 25.5 x 10^3 and 51 x 10^3, respectively, (a, b, c) stained with DAPI (blue nuclei), (d, e, f) stained with phalloidin (red cytoskeleton) and (g, h, i) the merge of DAPI and phalloidin images. Scanning electron microscopy of the cells and the PLGA fibers of MSC at 8.5 x 10^3 (j), 25.5 x 10^3 (k) and 51 x 10^3 (l). Representative micrographs of three individual experiments. a-i: 100x magnification.

The architecture of scaffolds used for tissue engineering is of critical importance to cell adhesion, attachment, growth, proliferation and metabolic activity. Scaffolds should have an interconnected pore structure and high porosity to ensure cellular penetration and adequate diffusion of nutrients to cells within the construction and to the extra-cellular matrix formed by these cells. Furthermore, a porous interconnected structure is required to allow diffusion of waste products out of the scaffolds and the

products of scaffold degradation should be able to leave the body without interference with other organs and surrounding tissue (O`Brien *et al* 2011). This study has shown that electrospun PLGA fibers were able to provide these properties.

3.6. Differentiation of cells on the scaffolds

Scaffolds in regenerative medicine for cartilage and bone engineering strategies have been shown in this study. The capacity of osteogenic and chondrogenic differentiation of stem cells was performed on the scaffolds (3D printed PCL matrices coated with PLGA electrospun nanofibers). The cells were able to perform osteogenic and chondrogenic differentiation on the scaffolds.

UCMSC on the scaffolds which underwent the osteogenic differentiation protocol expressed the osteogenic genes osteocalcin and osteopontin (figure 8a). The osteogenic differentiated cells on the scaffolds showed positive activity for alkaline phosphatase (figure 8b). Figure 8c shows the macroscopic aspect of undifferentiated control (left) and osteogenic differentiation (right) on the scaffolds produced. Photomicrographs by an optical microscope of control cells on the scaffolds without evidence of the calcified matrix stained with alizarin red S (figure 8d) and cryosectioned (figure 8e) and osteogenic differentiated of UCMSC staining by alizarin red S indicated by the red staining of deposited calcium (figure 8f) and cryosectioned (figure 8g).

The absence of chondrogenic differentiation in the controls was demonstrated by staining with alcian blue without blue staining of glycosaminoglycans deposits at figure 8h (left), figure 8i and 8j (cryosectioned) and the chondrogenic differentiation was demonstrated by blue staining of glycosaminoglycans deposits with alcian blue macroscopically at figure 8h (right), microscopically (figure 8k) and cryosectioned (figure 8l).

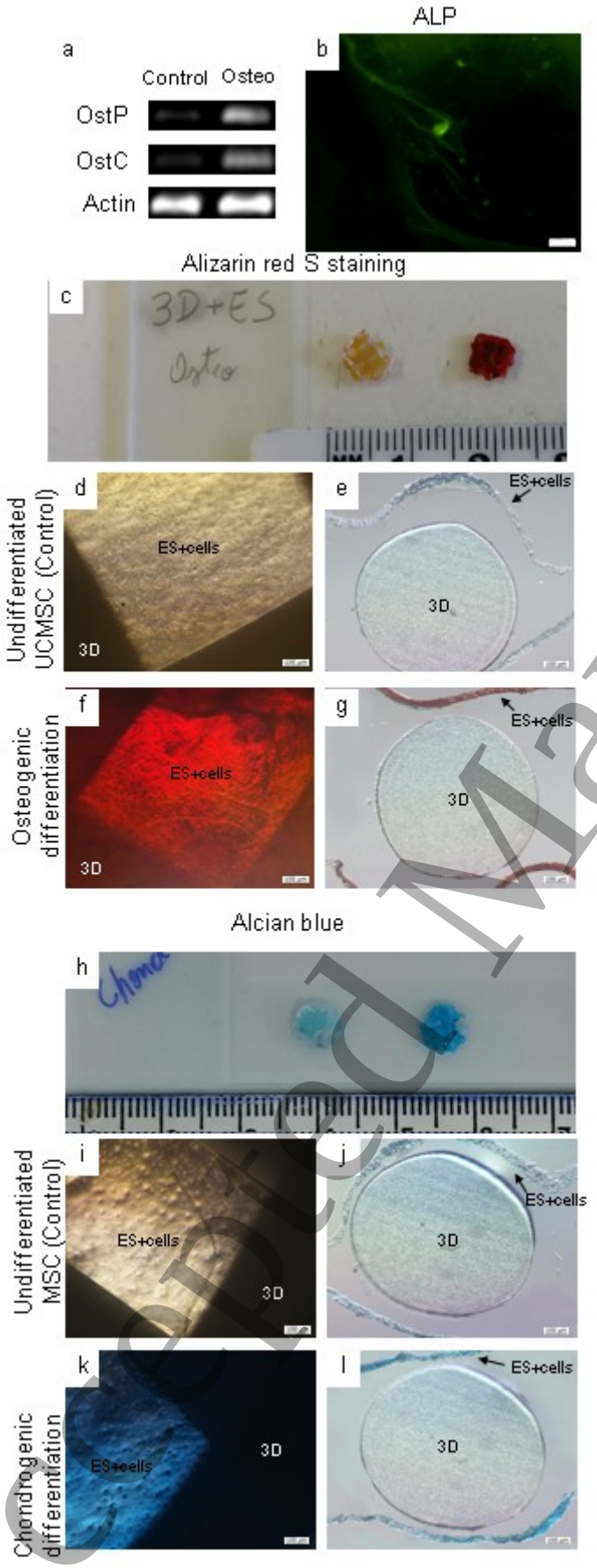

Figure 8. Osteogenic and chondrogenic differentiation of UCMSC on scaffolds (3D printed PCL matrices coated with PLGA electrospun nanofibers). a-f: osteogenic differentiation. (a) PCR; (b) alkaline phosphatase positive activity; c, d, e, f and g: alizarin red S staining on 3D+ES scaffolds. (c) macroscopic aspect of 3D+ES with UCMSC undifferentiated (left) and differentiated (right); (d) scaffolds with undifferentiated cells (osteogenic control); (e) cryosections of undifferentiated tissue constructs (osteogenic control); (f) osteogenic differentiation in scaffolds; (g) cryosection of osteogenic differentiation. h-l: chondrogenic differentiation alcian blue staining. (h) macroscopic aspect of 3D+ES with UCMSC undifferentiated (left) and differentiated (right); (i) scaffolds with undifferentiated cells (chondrogenic control); (j) chondrogenic differentiation on scaffolds; (k) cryosections of undifferentiated tissue constructs (chondrogenic control); (l) cryosection of chondrogenic differentiation.

3D: 3D printed matrix; ES: electrospun PLGA nanofibres. OsteoC: osteocalcin; OsteoP: osteopontin. b, d, e, f, g, i, j, k and l: 100x magnification.

3.7. Mechanical test of cells on the scaffolds

The results of mechanical properties of the scaffolds composed of PCL 3D printed matrix (3D), scaffolds 3D covered with electrospun PLGA nanofibers (3D+ES) and 3D+ES with seeded stem cells from umbilical cord (3D+ES+SC) are shown in table 2 and figure 9.

Table 2. Mechanical properties (average values and standard deviations) of 3D printed matrices (3D), 3D printed PCL matrices coated with PLGA electrospun nanofibers (3D+ES); and cells on the scaffolds (3D+ES+SC).

Sample	3D	3D+ES	3D+ES+SC
Young modulus (MPa)	20.72 ± 6.54	19.57 ± 2.43	18.53 ± 0.80
Tensile at break (MPa)	2.59 ± 0.45	2.60 ± 0.03	2.53 ± 0.21
Elongation at break (%)	73 ± 17	65 ± 9	74 ± 20

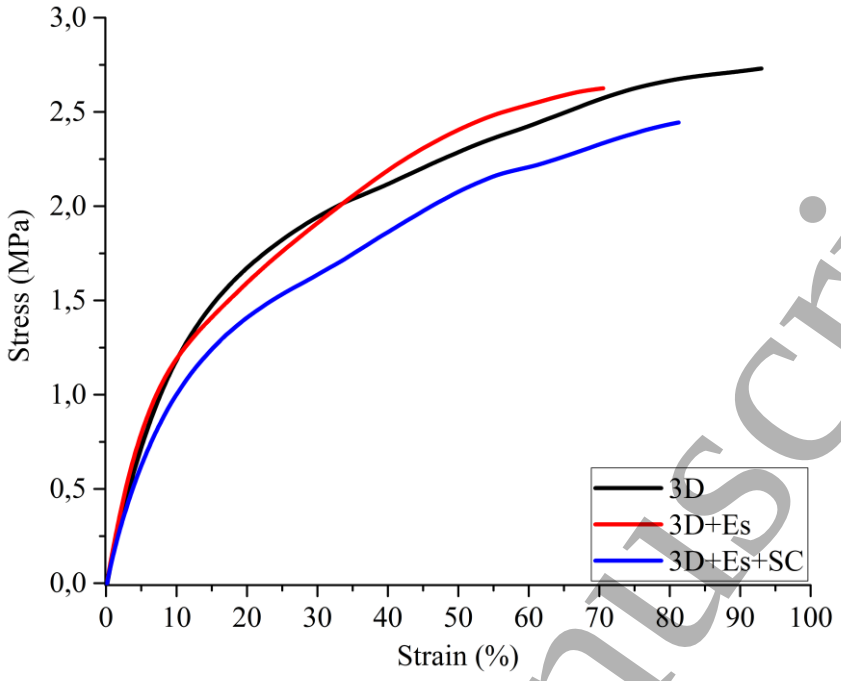

Figure 9. Mechanical properties of scaffolds. The 3D curve represents printed PCL matrices with the absence of nanofibers and cells; 3D+ES represents the 3D printed PCL matrices coated with PLGA electrospun nanofibers; and 3D+ES+SC are the scaffolds containing nanofibers and cells.

The results indicate typical stress x strain curves of scaffolds. The tensile properties indicate that the strength and modulus were not significantly affected by the electrospinning process or the cell cultivation in comparison with neat PCL 3D matrices. Nevertheless, for the scaffolds submitted to cell cultivation, a tendency of depletion of tensile at break and Young modulus was observed (blue line), indicating that the culture media might affect the mechanical properties. Although the cells used in the experiment could promote bone regeneration, no differences were observed in the mechanical properties. In order to investigate the scaffold reinforcement promoted by bone tissue formation, more extensive experiments are required.

However, the fibrous scaffolds produced by electrospinning are thin. The thickness of the PLGA fiber scaffolds produced by this group is about 37

μm (Acasigua *et al* 2014). Moreover, ideally, the scaffold should have mechanical properties consistent with the anatomical site into which it is to be implanted and, from a practical perspective, it must be strong enough to allow surgical handling during implantation (O`Brien *et al* 2011). The PCL matrices produced in this work were able to provide mechanical stability to the scaffolds.

Recently, several articles have focused on the fabrication of hybrid scaffolds for potential tissue engineering applications (Hoque *et al* 2011). Electrospinning may be combined with other scaffold fabrication technologies to compensate for its potential limitations, such as inadequate mechanical strength for load-bearing applications (O`Brien *et al* 2011). This was the strategy used in this work by combining support with greater mechanical stability due to the presence of 3D printed PCL matrices deposited in the filament and the electrospun PLGA fibers, which allows for better cell adhesion. The scaffolds are suitable for use in cell therapy and also for tissue regeneration purposes.

4. Conclusions

The combined polymeric structure used in this study made it possible to produce a support of PCL with controlled design and three-dimensional print. Moreover, it increased cell adhesion due to the PLGA nanostructured fibers which mimicked the extracellular matrix and which did not present cytotoxicity. The cells were shown to be viable and they adhered to the 3D+ES scaffolds. This hybrid scaffold produced by electrospun PLGA fibres coated with cells on both sides of the 3D structure can be used in cell therapy and regeneration of hard tissue.

Acknowledgements

The authors would like to acknowledge the support of the National Council of Technological and Scientific Development (CNPq),

Coordination for the Improvement of Higher Education Personnel (CAPES), Research Support Foundation of Rio Grande do Sul (FAPERGS), Research Support Foundation of São Paulo (FAPESP), the Stem Cell Research Institute (IPCT - Instituto de Pesquisa com Células-tronco) and INCT-BIOFABRIS. NM is thankful to the Fapergs/CAPES for the DOCFIX postdoctoral fellowship.

References

Acasigua G A X, Bernardi L, Braghirolli D I, Sant'ana Filho M, Pranke P and Fossati A C M 2014 Nanofiber scaffolds support bone regeneration associated with pulp stem cells *Curr. Stem Cell Res. Ther.* **9** 330-7

Açil Y, Zhang X, Nitsche T, Möller B, Gassling V, Wiltfang J and Gierloff M 2014 Effects of different scaffolds on rat adipose tissue derived stroma cells *J Craniomaxillofac Surg* **42** 825-34

Andrade J M M, Biegelmeyer R, Dresch R, Pereira D, Maurmann N, Pranke P, Henriques A T 2016 In vitro Antioxidant and Enzymatic Approaches to Evaluate Neuroprotector Potential of Blechnum Extracts without Cytotoxicity to Human Stem Cells. *Pharmacognosy Magazine* **12** 171-7

Ayres M, Ayres Jr M, Ayres D L and Santos A S 2007 *BioEstat 5.0. Aplicações estatísticas nas áreas das ciências biológicas e médicas* Belém: Instituto de Desenvolvimento Sustentável Mamirauá (IDSM)/MCT/CNPq) pp 364

Baksh D, Yao R and Tuan R S 2007 Comparison of proliferative and multilineage differentiation potential of human mesenchymal stem cells derived from umbilical cord and bone marrow *Stem Cells* **25** 1384-92

Barnes C P, Sell S A, Boland E D, Simpson D G and Bowlin G L 2007 Nanofiber technology: designing the next generation of tissue engineering scaffolds *Adv. Drug Deliv. Rev.* **59** 1413-33

Baume A S, Boughton P C, Coleman N V and Ruys A J 2016 Chapter 10 - Sterilization of tissue scaffolds. *Characterisation and Design of Tissue Scaffolds. Woodhead Publishing Series in Biomaterials* (Cambridge: Elsevier) pp 225-44

Callister W D 2007 Chapter 15 - Characteristics, Applications, and Processing of Polymers *Materials Science and Engineering: An Introduction* (New York: John Wiley & Sons, Inc) **7** pp 523-76

Chan B P and Leong K W 2008 Scaffolding in tissue engineering: general approaches and tissue-specific considerations *Eur. Spine. J.* ***17*** *467*-79

Chua C K and Yeong W Y 2015 Chapter 1 Introduction to Tissue Engineering In *Bioprinting: principles and applications* (Singapore: World Scientific Publishing Co. Pte. Ltd.) **1** pp 1-15

Cui X, Chen L, Xue T, Yu J, Liu J, Ji Y and Cheng L 2015 Human umbilical cord and dental pulp-derived mesenchymal stem cells: biological characteristics and potential roles in vitro and in vivo *Mol Med Rep* **11** 3269-78

Dalton P D, Vaquette C, Farrugia B L, Dargaville T R, Brown T D and Hutmacher D W 2013 Electrospinning and additive manufacturing: converging technologies *Biomater. Sci.* **1** 171-85

Dhandayuthapani B, Yoshida Y, Maekawa T, and Kumar D S 2011 Polymeric Scaffolds in Tissue Engineering Application: A Review *Int. J. of Polymer Science* **2011** 290602

Dominici M, Le Blanc K, Mueller I, Slaper-Cortenbach I, Marini F, Krause D, Deans R, Keating A, Prockop Dj and Horwitz E 2006 Minimal criteria for defining multipotent mesenchymal stromal cells. The International Society for Cellular Therapy position statement *Cytotherapy* **8** 315-7

Giannitelli S M, Mozetic P, Trombetta M and Rainer A 2015 Combined additive manufacturing approaches in tissue engineering *Acta Biomaterialia* **24** 1-11

Hollister S J 2005 Porous scaffold design for tissue engineering *Nature Mater* **4** 518-24

Hoque M E, Meng T T H , Chuan Y L, Chowdhury M and Prasad R G S V 2014 Fabrication and characterization of hybrid PCL/PEG 3D scaffolds for potential tissue engineering applications *Materials Letters* **131** 255-8

Hussein K H, Park K M, Kang K S and Woo H M 2016 Biocompatibility evaluation of tissue-engineered decellularized scaffolds for biomedical application *Materials Science and Engineering: C* **67** 766-78

Inforçatti Neto P, Lixandrão A, Pereira F D A S, Silva J, Silveira Z 2011 Thermoplastic filament extruder head for desktop Additive Manufacturing machines *Innovative Developments in Virtual and Physical Prototyping: Proceedings of the 5th International Conference on Advanced Research in Virtual and Rapid Prototyping* (Leiden: CRC Press / Balkema, Taylor & Francis Group) **1** pp 635-8

Kang S K, Shin I L, Ko M S, Jo J Y and Ra J C 2012 Journey of mesenchymal stem cells for homing: strategies to enhance efficacy and safety of stem cell therapy *Stem Cells Int.* **2012** 342968

Kern S, Eichler H, Stoeve J, Kluter H and Bieback K 2006 Comparative analysis of mesenchymal stem cells from bone marrow, umbilical cord blood, or adipose tissue *Stem Cells* **24** 1294-301

Langer R and Vacanti J P 1993 Tissue engineering *Science* **260** 920-6

Lavoie J R and Rosu-Myles M 2013 Uncovering the secretes of mesenchymal stem cells *Biochimie* **95** 2212-21

Lixandrão A L, Cheung P Y C, Noritomi P Y, da Silva J V L, Colangelo N, Kang H, Lipson H, Butcher J T, Malone E and Inforçatti Neto P 2009 Construction and Adaptation of an Open Source Rapid Prototyping Machine for Biomedical Research Purposes - a Multinational Collaborative Development *Innovative Developments in Design and Manufacturing: Advanced Research in Virtual and Rapid Prototyping* (Leiden: CRC Press / Balkema, Taylor & Francis Group) pp 469-73

Minuth W W, Strehl R and Shumacher K 2005 5 - Concepts of Tissue Creation *Tissue Engineering: Essentials for Daily Laboratory Work* (Weinheim: Wiley-VCH) pp 130-90

Moretti P, Hatlapatka T, Marten D, Lavrentieva A, Majore I, Hass R and Kasper C C 2010 Mesenchymal stromal cells derived from human umbilical cord tissues: primitive cells with potential for clinical and tissue engineering applications *Adv Biochem Eng Biotechnol* **123** 29-54

O'Brien F J 2011 Biomaterials & scaffolds for tissue engineering *Materials Today* **14** 88-9

Paul G and Anisimovc S V 2013 The secretome of mesenchymal stem cells: potential implications for neuroregeneration *Biochimie* **95** 2246-56

Ramakrishna S, Fujihara K, Teo W E, Lim T C and Ma Z 2005 Basics relevant to Electrospinning *An Introduction to Electrospinning and Nanofibers* (Singapore: World Scientific) pp 63-80

Rana D, Arulkumar S, Vishwakarma A and Ramalingam M 2015 Chapter 10 - Considerations on Designing Scaffold for Tissue Engineering. *In Stem Cell Biology and Tissue Engineering in Dental Sciences* (Boston: Academic Press) pp 133-148

Rocha A M, Quintella C M and Torres E A 2012 Prospecção de artigos e patentes sobre polímeros biocompatíveis aplicados à engenharia de tecidos e medicina regenerativa. *Cadernos de Prospecção* **5** 72-85

Schwartz M A and Assoian R K 2001 Integrins and cell proliferation: regulation of cyclin-dependent kinases via cytoplasmic signaling pathways *J Cell Sci* **114** 2553-60

Skardal A and Atala A 2015 Biomaterials for integration with 3-D bioprinting *Ann. Biomed. Eng.* **43** 730-46

Teo W E, He W and Ramakrishna S 2006 Electrospun scaffold tailored for tissue-specific extracellular matrix *Biotechnol. J.* **1** 918-29

Ulery B D, Nair L S and Laurencin C T 2011 Biomedical Applications of Biodegradable Polymers *J. Polym. Sci. B. Polym. Phys.* **49** 832-64

Ullah I, Subbarao R B and Rho G J 2015 Human mesenchymal stem cells - current trends and future prospective *Biosci. Rep*. **35** e00191

Weldon C B, Tsui J H, Shankarappa S A, Nguyen V T, Ma M, Anderson D G and Kohane D S 2012 Electrospun drug-eluting sutures for local anesthesia *J Control Release* **161** 903-9

Zanatta G, Rudisile M, Camassola M, Wendorff J, Nardi N, Gottfried C, Pranke P and Netto C A 2012 Mesenchymal Stem Cell Adherence on Poly(D, L-Lactide-Co-Glycolide) Nanofibers Scaffold is Integrin-β1 Receptor Dependent *J. Biomed Nanotechnol.* **8** 211-8